Ohmic decay of magnetic flux expelled from neutron star interiors

D. Bhattacharya[1] and B. Datta[1,2]

[1]*Raman Research Institute, Bangalore 560080, India*
[2]*Indian Institute of Astrophysics, Bangalore 560034, India*

ABSTRACT

We study Ohmic diffusion of magnetic flux expelled from the superconducting core of a neutron star to its crust owing to spindown-induced field evolution. We find that Ohmic decay time-scales in the range $10^{7.5}$–10^9 yr obtain for a wide range of crustal temperatures and impurity concentrations for various equation of state models of neutron star matter. This result is in agreement with the Ohmic time-scale that appears to be required to explain observed magnetic field strengths of isolated and binary neutron stars in the spindown-induced magnetic flux expulsion scenario.

Key words: magnetic fields – stars: neutron – pulsars: general.

1 INTRODUCTION

The evolution of magnetic fields of neutron stars has been a focus of much research interest, motivated by the realization that this plays an essential role in a variety of observed pulsar phenomena. There is, however, no consensus at present on the physical mechanism responsible for the field evolution. However, all suggested mechanisms rely on physical processes in the neutron star crust for final reduction of the surface magnetic field. The relevant physical processes in the crust include Ohmic dissipation, ambipolar diffusion, Hall drift, etc. (see e.g. Goldreich & Reisenegger 1992). In recent times there have been several calculations addressed specifically to the problem of the Ohmic decay of neutron star crustal magnetic field. The first of these was by Sang & Chanmugam (1987). These authors did not include the cooling of the neutron star in their calculations. The variation of the temperature in the interior of neutron stars with respect to the age of the star is, however, important, as this significantly affects the electrical conductivity of the crustal material. In a later calculation, Sang, Chanmugam & Tsuruta (1990) included the cooling effect, adopting a model due to Nomoto & Tsuruta (1987). Similar computations, but using other cooling models for neutron stars, have been reported by Urpin & Muslimov (1992) and Urpin & van Riper (1993). These calculations are suggestive of some form of power-law field decay with time rather than the exponential decay suggested by Gunn & Ostriker (1970).

The spin evolution of pulsars may be an important factor for their magnetic field decay (Chanmugam 1984). A promising model in this category is that suggested by Srinivasan et al. (1990). This involves the interpinning of the quantized flux tubes and the quantized vortices of superfluid neutron matter in the neutron star interior. The final field decay that can be achieved in this model is strongly dependent on the field diffusion time-scales across the neutron star crust (Jahan Miri & Bhattacharya 1994). In order to obtain constraints on the Ohmic diffusion time-scale, Jahan Miri &

Bhattacharya (1994) examined the evolution of a neutron star magnetic field in a low-mass binary, owing to the interaction of its magnetosphere with the stellar wind of the companion. These authors concluded that the low magnetic fields of millisecond pulsars may be accounted for by this mechanism, if the Ohmic time-scale lies in the range $10^8 - 10^9$ yr. However, this time-scale so far has not been estimated on the basis of the crustal physics. In this paper we attempt to do so.

Specifically, we study here Ohmic diffusion of the magnetic field that has just been expelled from the interior of a neutron star and deposited in the bottom layers of the stellar crust (see Srinivasan et al. 1990). This work differs from all previous studies of crustal magnetic field evolution (e.g. Sang & Chanmugam 1987; Urpin & Muslimov 1992; Urpin & van Riper 1993; Urpin, Chanmugam & Sang 1994; Geppert & Urpin 1994; Urpin & Geppert 1995) in the fact that these other studies assume the initial magnetic field to be confined to the very outer layers of the crust. Since, in our case, the currents supporting the field are located deep inside the stellar crust, we find that a major factor that influences the evolution is the impurity parameter of the crust lattice. No quantitative estimate of this parameter is, however, available. So, we perform here model calculations for a wide range of values of the crust impurity parameter. We also study in this paper the dependence of the field evolution on the equation of state of the neutron star matter.

2 THE FIELD EVOLUTION

The evolution of the magnetic field $\boldsymbol{B}$ with time, assuming Ohmic dissipation, is given by

$$\frac{\partial \boldsymbol{B}}{\partial t} = -\nabla \times \left(\frac{c^2}{4\pi\sigma} \nabla \times \boldsymbol{B} \right), \tag{1}$$

where σ is the electrical conductivity of the material across which the Ohmic diffusion takes place. We shall assume this magnetic field to be a pure dipole field. For computational convenience, we

shall describe the field by means of the function $g(x,t)$, where $x = r/R$ is the ratio of the radial coordinate to the stellar radius and t stands for time. This function can be written in terms of the vector potential $A = (0, 0, A_\phi)$ as

$$A_\phi = g(x,t) \sin\theta / r \qquad (2)$$

using spherical polar coordinates. The field evolution equation then becomes

$$\frac{\partial^2 g(x,t)}{\partial x^2} - \frac{2}{x^2} g(x,t) = \frac{4\pi R^2 \sigma}{c^2} \frac{\partial g(x,t)}{\partial t}. \qquad (3)$$

Solution of equation (3) with the boundary conditions (valid for all times)

$$\frac{\partial g}{\partial x} + \frac{g}{x} = 0 \text{ at } x = 1, \qquad (4)$$

$$g = 0 \text{ at crust bottom} \qquad (5)$$

provides the magnetic field decay with age.

3 THE MODEL DETAILS

3.1 The initial profile

In the literature on this topic, the profile for the initial magnetic field has been considered to correspond to post-formation field generation. These profiles are taken to be confined to a very narrow region close to the surface of the neutron star. We assume a different type of initial field distribution, appropriate for the field expulsion from the interior and deposition at the crust bottom, given by

$$g(x,0) = \frac{1}{\sqrt{2\pi}} \int_{-\infty}^{x} e^{-(x'-x_0)^2/2x_w^2} \, dx'. \qquad (6)$$

This function varies from nearly unity to nearly zero within a width x_w around $x = x_0$. We choose x_0 to be near the bottom of the crust and x_w to be of the order of 0.01.

3.2 The electrical conductivity

The electrical conductivity of the neutron star crustal material is determined mainly by the following two factors: the scattering of electrons by phonons and the scattering of electrons by impurities in the crust lattice.

We compute the phonon scattering conductivity σ_{ph} using the method of Itoh et al. (1984) and the impurity scattering conductivity σ_{imp} using expressions derived by Yakovlev & Urpin (1980). The net conductivity of the crustal material at a given depth is then computed as

$$\sigma = \left(\frac{1}{\sigma_{ph}} + \frac{1}{\sigma_{imp}} \right)^{-1}. \qquad (7)$$

In the above, σ_{ph} is a function of the local temperature and σ_{imp} is inversely proportional to the impurity parameter Q, defined as

$$Q = \frac{1}{n} \sum_i n_i (Z - Z_i)^2, \qquad (8)$$

where n and Z are the density and electrical charge of background ions in the crust lattice without impurity, and Z_i and n_i are the charge and density of the ith impurity species. The sum in equation (8) extends over all species of impurity. There is no a priori knowledge of what the value of the parameter Q should be in neutron star

crusts. We therefore use a range of Q-values in our computations, and discuss the sensitivity of the results to this parameter.

3.3 The temperature distribution

Following Gudmundsson, Pethick & Epstein (1983), we assume an isothermal neutron star crust. These authors suggested the following empirical relationship between the interior temperature T_i and the crust surface temperature T_s for neutron stars:

$$T_i = 1.288 \times 10^8 (T_{s6}^4 / g_{s14})^{0.455}, \qquad (9)$$

where T_{s6} is the surface temperature in units of 10^6 K and g_{s14} is the surface gravity in units of 10^{14} cm s^{-2}. This expression is expected to be valid for interior temperatures $\gtrsim 10^6$ K. We shall consider here the following two possibilities for the temperature distribution: (i) the surface temperature evolves as in the case of an isolated neutron star and the interior temperature follows it in accordance with equation (9); and (ii) the interior temperature has a fixed, constant value throughout the evolution of the magnetic field. For case (i), we adopt the neutron star cooling model as given by van Riper (1991), for a 1.4-$M_\odot$ neutron star configuration and corresponding to the Friedman–Pandharipande equation of state. Cooling models corresponding to each individual neutron star equation of state model are not available in the literature. So, for our purpose here we use the same cooling curve as mentioned above for the other equations of state. For case (ii), we consider the following fixed temperatures: 10^8, 10^7 and 10^6 K.

4 CHOICE OF THE EQUATION OF STATE (EOS)

The structure of neutron stars depends sensitively on the EOS at high densities, especially for densities $\gtrsim 2.4 \times 10^{14}$ g cm^{-3}. In general, the stiffer the EOS, the larger the crustal thickness for a given neutron star mass. This has a direct bearing in the present context, since the crustal thickness is an important deciding factor for the time required for Ohmic diffusion of the magnetic field. The EOS is determined by the composition of neutron star matter, which depends on the density. The composition of degenerate matter in neutron star interiors is expected to be dominated by neutrons, in addition to small amounts of protons, electrons and muons. Admixtures of other elementary particles, such as pions and hyperons, have also been suggested. A persistent problem in determining the EOS at high densities ($\sim 10^{15}$ g cm^{-3}) is what to choose for the interaction among the strongly interacting particles. All calculations involve extrapolations from known nuclear matter properties (which correspond to a density of about 2.4×10^{14} g cm^{-3}) in some form or other. For our purpose here, we have selected from the literature a set of five EOS models that are based on representative neutron star matter interaction models. This choice is not exhaustive, but it serves to illustrate the role of the EOS in the evolution of neutron star magnetic fields. A brief description of these EOS models is given below.

(1) Bethe–Johnson model. Bethe & Johnson (1974) devised phenomenological potentials for nucleon–nucleon interaction, and used these to derive the EOS of high-density matter. The many-body method used to compute the EOS is the lowest order constrained variational method that was suggested by Pandharipande (1971). We have chosen here the Bethe–Johnson model V, which corresponds to pure neutron matter.

(2) Walecka model. Walecka (1974) gave an EOS for pure neutron matter at high densities based on a relativistic approach,

using scalar and vector meson exchange interactions. The masses and the coupling constants of the mesons were adjusted to reproduce the saturation property of equilibrium nuclear matter.

(3) Friedman–Pandharipande model. This EOS (Friedman & Pandharipande 1981) is also based on the lowest order constrained variational method. An improved phenomenological nucleon–nucleon potential, which incorporates three-body correlations, is used. EOSs for pure neutron matter as well as nuclear matter are derived. We use here the former.

(4) Wiringa–Fiks–Fabrocini model. Wiringa, Fiks & Fabrocini (1988) gave an EOS for dense nuclear as well as neutron matter which is similar to the Friedman–Pandharipande model, but is an improvement over it in that the long-range attraction term in the interaction Hamiltonian is treated better. The authors have given three different models. We consider here the model UV14 + UVII (neutrons, protons, electrons and muons in beta equilibrium).

(5) Chiral sigma model. Sahu, Basu & Datta (1993) derived a field theoretical EOS for high-density matter, assuming the composition to be neutron-rich matter in beta equilibrium, based on the chiral sigma model. This model includes an isoscalar vector meson field generated dynamically. It reproduces the empirical values of the saturation density and binding energy of equilibrium nuclear matter, and also gives the right isospin symmetry coefficient for asymmetric nuclear matter (by incorporating the interaction due to the isospin triplet ρ meson). The energy per nucleon of nuclear matter shows good agreement with estimates inferred from heavy ion collision data.

An EOS is said to be stiff if for a given density there is more repulsion among the constituent particles, and hence a larger net pressure. In contrast, a soft EOS will mean more attraction in the pressure term. The stiffer the EOS, the larger the crust thickness for a given neutron star mass (Datta, Thampan & Bhattacharya 1995). Among the above EOS models, the ones due to Walecka (1974) and Sahu et al. (1993) are quite stiff, whereas the rest are comparatively soft EOSs.

5 RESULTS AND DISCUSSION

In order to solve equation (3), it is necessary to know the variation of the density across the neutron star crust. In an earlier paper (Datta et al. 1995), we have reported accurate computations of neutron star crustal density profiles for several EOS models. We use those results here to calculate the crustal magnetic field evolution for a 1.4-$M_\odot$ neutron star configuration. We solve equation (3) numerically using the Crank–Nicholson method. We have checked the accuracy of our numerical program by reproducing the field evolution results reported by Urpin & van Riper (1993).

In solving equation (3), we have followed the field evolution for 10^{10} yr under the following conditions: (i) the impurity parameter Q is taken to vary from 10^{-3} to 0.1; and (ii) a temperature variation range of 10^8–10^6 K for all the EOS models as mentioned in Section 4, and for a wide range of values of the width parameter x_w. The main results of our calculations are illustrated in Figs 1–4.

Fig. 1 shows a typical initial profile of the function $g(x, t)$ adopted for our calculations. Fig. 2 shows the time evolution of the surface field for different assumed values of Q and corresponding to the Wiringa–Fiks–Fabrocini EOS. In Fig. 3 we have compared the final surface field after a 10^{10}-yr evolution period, for different values of Q and different EOS models. Both Figs 2 and 3 display evolution assuming the van Riper (1991) model for neutron star cooling. The onset of the field evolution is assumed to be coincident
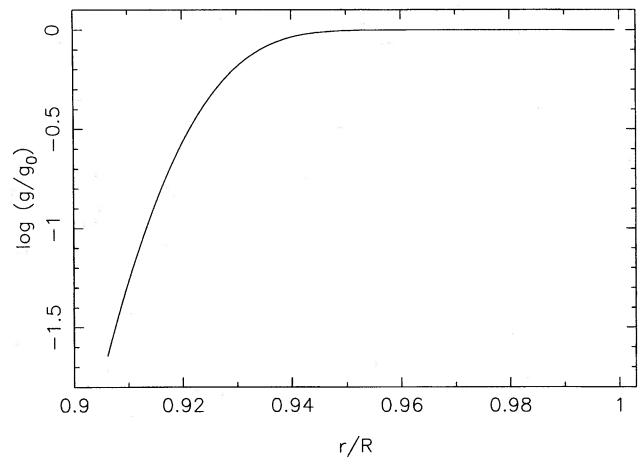
Figure 1. The assumed initial profile of the function g defined in equation (2). The shape has been chosen to model the distribution of magnetic flux immediately after expulsion from the superconducting interior. The value of g is nearly constant over most of the crust, and then rapidly falls to zero at the bottom of the crust ($r/R \sim 0.9$). r is the distance from the centre of the star and R is the radius of the neutron star. g_0 is the value of g at the stellar surface.

with the onset of the cooling of the neutron star. This corresponds to the case where the field expulsion takes place very early in the life of the neutron star. We have also explored cases where the field expulsion occurs much later in the cooling history – delayed by up to 10^7 yr, by which time the interior temperature has fallen to a very low value. However, we find that the results corresponding to such delayed expulsion are nearly identical to those shown in Fig. 2, differing by less than ~3 per cent in all cases. This illustrates the fact that Ohmic diffusion of the expelled field is determined mainly by the impurity parameter and not by the temperature in a cooling neutron star. In Fig. 4 we present results for constant assumed values of the interior temperature, corresponding to the Wiringa–Fiks–Fabrocini EOS and $Q = 0.01$. The constant assumed temperatures are 10^8,
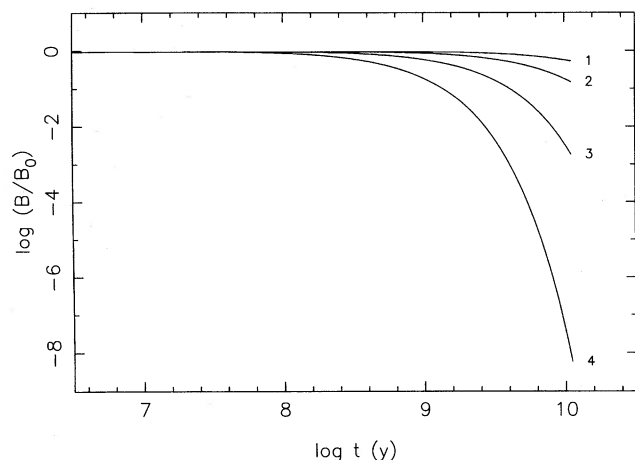
Figure 2. The evolution of the surface field strength B for the equation of state of Wiringa et al. (1988). It is assumed that the surface temperature of the star follows the normal matter cooling curve as computed by van Riper (1991). The evolution is dominated by resistivity arising from impurity scattering. Curves corresponding to four different values of the impurity strength parameter Q are shown: (1) $Q = 0.001$, (2) $Q = 0.003$, (3) $Q = 0.01$ and (4) $Q = 0.03$. B_0 is the initial surface field strength.
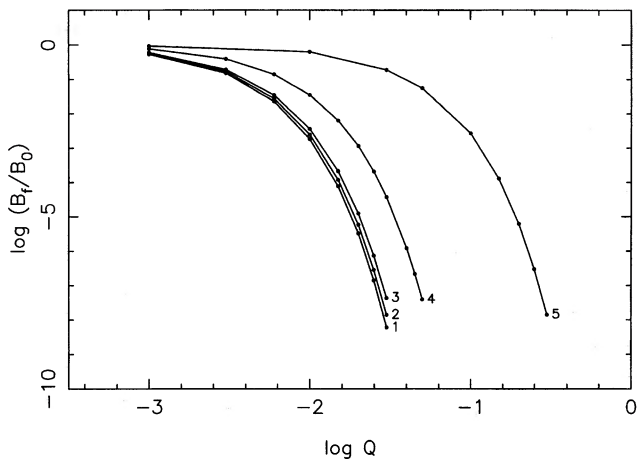
© 1996 RAS, MNRAS **282**, 1059–1063

Figure 3. The final surface field strength after an evolution lasting 10^{10} yr. The dependence of the evolution on the crustal impurity parameter Q is shown for different equations of state: (1) Wiringa et al. (1988), (2) Friedman & Pandharipande (1981), (3) Bethe & Johnson (1974), (4) Walecka (1974) and (5) Sahu et al. (1993). It is clearly seen that the surface field decays faster for softer equations of state, which correspond to smaller crustal thickness.

10^7 and 10^6 K. These constant, and somewhat high, values of the interior temperature are likely to occur if the neutron star undergoes steady accretion on its surface (Miralda-Escudé, Haensel & Pac-zyński 1990; Zdunik et al. 1992) We find that the field evolution characteristics are insensitive to variations with respect to (i) the width parameter x_w and (ii) the temperature, provided that the interior temperature is less than 10^6 K. The latter result is easily understood because, for this temperature regime, it is the impurity scattering that plays the dominant role in deciding the conductivity. The effective e-folding 'decay time' τ in the case when the neutron star starts off hot, and cools according to the standard cooling law, is found to lie in the range 10^8–10^9 yr for the moderately soft equations of state considered here (see Fig. 2). For higher interior temperatures, τ has smaller values. If the interior temperature is of

the order of 10^8 K and constant, we find that τ is about $10^{7.5}$ yr (see Fig. 4).

The impurity parameter Q has a significant effect on the field evolution time-scales, particularly for higher values of Q. The impurity scattering cross-section increases with Q, and is independent of temperature. For high values of Q, it is the dominating factor in determining the electrical conductivity, and hence the Ohmic dissipation time-scale. This feature is brought out in Fig. 3. It should be mentioned here that, once the field starts decaying, the decay proceeds in a manifestly non-exponential manner, as is evident from Figs 2 and 4. Therefore, strictly speaking, the decay time τ has a limited meaning, and should be thought of as the first e-folding time.

Fig. 3 shows that the results corresponding to the Bethe–Johnson, Friedman–Pandharipande and Wiringa–Fiks–Fabrocini EOS models are quite similar. These are the equations of state that possess similar 'stiffness'. The other two EOS models are quite stiff, and so give large values for the thickness of the neutron star crust. In such cases, the diffusion must cover a larger distance before the effect of the flux expulsion is 'visible' at the stellar surface. Consequently, the field decay time-scales for these EOSs are expected to be large. This is clearly depicted in Fig. 3.

It may be noted here that the initial g-profile that we have assumed decreases monotonically from the neutron star surface to the crust bottom. However, it may well be that soon after the expulsion of the flux from the interior of the neutron star, its accumulation at the bottom of the crust may produce a maximum in the initial g-profile close to the crust bottom. To explore the possible effects of this on the evolution of the surface field, we have evolved a model with a Gaussian peaked at $x = x_0$ superposed on the initial profile given by equation (6) such that a maximum in initial g-profile of magnitude 10 times the surface value of g is produced at $x = x_0$. We find that this is reflected in the surface field evolution in the following manner. The surface field exhibits a slight enhancement before starting to decay. The decay time-scales are not modified, and the maximum deviation from the evolution shown in Fig. 2 is less than half an order of magnitude.

The work of Jahan Miri & Bhattacharya (1994) found that the best correspondence with observations for magnetic fields of neutron stars processed in low-mass binaries can be obtained if the Ohmic diffusion time-scale in the crust lies in the range 10^8–10^9 yr, the decay of the expelled field being described by an exponential with this time-scale for all neutron stars. As can be seen from the above, Ohmic time-scales in this range can be easily obtained for most equations of state if the impurity parameter Q is larger than ~0.01. For the stiffest of EOS models, however, one needs an impurity parameter an order of magnitude higher to achieve similar time-scales. The heating of the crust also has a significant influence on the rate of Ohmic diffusion – raising the temperature of the crust from 10^7 to 10^8 K can reduce the Ohmic time-scale by more than half an order of magnitude. Since the rate of accretion on the surface of the neutron star after the flux expulsion is likely to be quite different in different cases, resulting in different crustal temperatures, it seems unlikely that the same Ohmic time-scale would be applicable to all neutron stars. Therefore, in a more refined investigation of spindown-induced field evolution, one must take into account the accretion history on the neutron star in detail to estimate the final field strength.

As can be seen in the cases where Ohmic time-scales in the above range do obtain, the crustal field strength drops to very small fractions (about 10^{-7}–10^{-8}) of the original value in less than a Hubble time. In these cases, the external observer will 'experience'
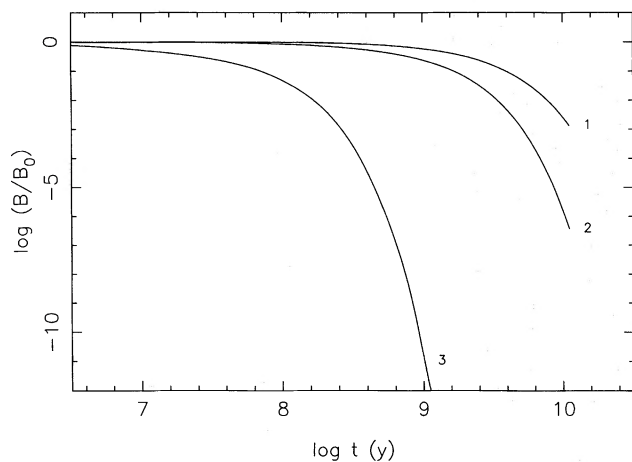

Figure 4. Evolution of the surface field strength under constant, elevated crustal temperature as might be expected when steady accretion takes place on the neutron star surface. The curves shown correspond to the equation of state of Wiringa et al. (1988) and a Q of 0.01. The assumed temperatures of the inner crust are: (1) 10^6 K, (2) 10^7 K and (3) 10^8 K. Comparison with Fig. 2 shows clearly a more rapid drop in the field strength in this case.

only the residual, unexpelled magnetic field in the neutron star core which does not undergo Ohmic evolution, since the computations of Jahan Miri & Bhattacharya (1994) indicate that the maximum amount of magnetic flux expulsion achieved under these conditions still leaves about $(10^{-3}-10^{-4})$ of the original flux inside the neutron star core. Given the field evolution as discussed here, this would mean that neutron stars evolved in this way will possess final dipole magnetic field strengths of the order of 10^8-10^9 G, as seems to be observed in the lowest-field pulsars known. Jahan Miri & Bhattacharya (1994) showed that this lower limit follows from the maximum spindown that may occur in the coupled magnetic and spin evolution of the neutron star interacting with the stellar wind of its companion. The non-exponential nature of the decay, as found by us, might modify this result somewhat, particularly if the initial Ohmic time-scale is very long (10^9 yr or longer).

ACKNOWLEDGMENTS

REFERENCES

Bethe H.A., Johnson M.B., 1974, Nucl. Phys., A230, 1
Chanmugam G., 1984, in Reynolds S.P., Stinebring D.R., eds, Millisecond Pulsars. NRAO, Green Bank, p. 213
Datta B., Thampan A.V., Bhattacharya D., 1995, JA&A, 16, 375
Friedman B., Pandharipande V.R., 1981, Nucl. Phys., A361, 502
Geppert U., Urpin V., 1994, MNRAS, 271, 490
Goldreich P., Reisenegger A., 1992, ApJ, 395, 250
Gudmundsson E.H., Pethick C.J., Epstein R.I., 1983, ApJ, 272, 286
Gunn J.E., Ostriker J.P., 1970, ApJ, 160, 979
Itoh N., Kohyama Y., Matsumoto N., Seki M., 1984, ApJ, 285, 758
Jahan Miri M., Bhattacharya D., 1994, MNRAS, 269, 455
Miralda-Escudé J., Haensel P., Paczyński B., 1990, ApJ, 362, 572
Nomoto K., Tsuruta S., 1987, ApJ, 312, 711
Pandharipande V.R., 1971, Nucl. Phys., A174, 641
Sahu P.K., Basu R., Datta B., 1993, ApJ, 416, 267
Sang Y., Chanmugam G., 1987, ApJ, 323, L61
Sang Y., Chanmugam G., Tsuruta S., 1990, in Kundt W., ed., Neutron Stars and Their Birth Events. Kluwer, Dordrecht, p. 127
Srinivasan G., Bhattacharya D., Muslimov A.G., Tsygan A.I., 1990, Curr. Sci., 59, 31
Urpin V., Geppert U., 1995, MNRAS, 275, 1117
Urpin V.A., Muslimov A.G., 1992, MNRAS, 256, 261
Urpin V.A., van Riper K.A., 1993, ApJ, 411, L87
Urpin V.A., Chanmugam G., Sang Y., 1994, ApJ, 433, 780
van Riper K., 1991, ApJS, 75, 449
Walecka J.D., 1974, Ann. Phys., 83, 491
Wiringa R.B., Fiks V., Fabrocini A., 1988, Phys. Rev., C38, 1010
Yakovlev D.G., Urpin V., 1980, SvA, 24, 303
Zdunik J.L., Haensel P., Paczyński B., Miralda-Escudé J., 1992, ApJ, 384, 129